THE ASTRONOMICAL JOURNAL VOLUME 105, NUMBER 5 MAY 1993

# THE OPTICAL PROPERTIES OF LOW LUMINOSITY RADIO GALAXIES WITH RADIO JETS

J. I. GONZALEZ-SERRANO AND R. CARBALLO

Dpto. de Física Moderna, Universidad de Cantabria and Instituto de Estudios Avanzados en Física Moderna y Biología Molecular, CSIC-Universidad de Cantabria, Santander, Spain
Electronic mail: gserrano@ccucvx.unican.es, carbello@ccucvx.unican.es

I. PÉREZ-FOURNON

Instituto de Astrofísica de Canarias, Tenerife, Spain
Electronic mail: ipf@iac.es

*Received 1992 October 20; revised 1993 January 21*

## ABSTRACT

Broad-band CCD images of 24 low luminosity radio galaxies containing radio jets have been obtained to study their optical properties. Surface photometry of the galaxies was performed by fitting ellipses to the light distribution in order to obtain the surface brightness profile and the geometrical parameters of the galaxies. The optical morphology, the photometric parameters, and the local environment of the galaxies are discussed and compared with the results for other galaxy samples. The galaxies in this work have absolute magnitudes similar to bright cluster galaxies, and they are more luminous than powerful radio sources. They inhabit regions of higher galaxy density than powerful radio galaxies and radio-quiet ellipticals. A fraction as large as 75% of the galaxies show morphological peculiarities in the optical, indicating gravitational interaction with nearby companions and/or recent merging. We argue that low luminosity radio galaxies could be the precursors of cD galaxies in clusters or groups of galaxies, on the basis of their optical luminosity, the local environment, presence of extended envelopes, indications of merging processes, x-ray emission, and presence of dumbbell systems and multiple nuclei.

## 1. INTRODUCTION

Optical studies of radio galaxies over the last years have provided a better understanding of the structure and properties of their host galaxies and of the relation with their immediate environment. The optical data show evidence that low luminosity radio galaxies (LLRG), usually showing Fanaroff–Riley type I (FR I) radio morphology (Fanaroff & Riley 1974), and powerful radio galaxies (PRG), that generally show FR II morphology, are associated with different types of galaxies. A first major relation between radio luminosity/morphology and optical line emission was found by Hine & Longair (1979). Whereas that the photometric parameters of PRG appear similar to those of normal ellipticals, LLRG are more luminous and have shallower light profiles, resembling bright cluster galaxies (Smith & Heckman 1989a,b; Owen & Laing 1989). Heckman *et al.* (1985) found that LLRG are located in regions of higher local galaxy density than radio-quiet ellipticals. Lilly & Prestage (1987) and Heckman *et al.* (1986, hereafter H86) studied the environment of radio galaxies, mostly of intermediate or high power (total power at 1.4 GHz, $P_{1.4} \gtrsim 10^{25}$ W Hz$^{-1}$ ), and found that FR II sources are located in poorer environments than FR I sources, confirming the relation between radio luminosity/morphology and local galaxy density.

Optical surface photometry of radio galaxies led to the important idea of a link between radio activity and gravitational interaction and/or merging events. Although both PRG and LLRG have in common indications that gravitational interaction or merging have occurred in these systems, PRG seem to be associated with processes involving at least one disk galaxy whereas that the interactions in LLRG occur between elliptical galaxies (Colina & Pérez-Fournon 1990b). H86 found that a high fraction of powerful radio galaxies show morphological peculiarities in the form of tails, fans, bridges, dust features, and shells and present strong optical emission lines. From this evidence they conclude that these objects arise from disk–disk or disk–elliptical collisions. Studies of LLRG have shown that these galaxies have multiple nuclei, isophote distortions, and also present signatures of interaction or merging processes (Lilly & Prestage 1987; Colina & Pérez-Fournon 1990a,b; González-Serrano & Pérez-Fournon 1989, 1991, 1992). Since LLRG and their companions are early-type galaxies, the morphological signatures of interactions between two such dynamically-hot systems are usually rather subtle.

To study LLRG in more detail we have carried out CCD surface photometry of a sample of such galaxies in the Northern hemisphere. The sample is particularly important because optical studies have dealt mostly with samples of intermediate to high power radio sources. The present work is an extension of previous studies of individual radio galaxies belonging to a complete sample of LLRG with radio jets at the kpc scale (González-Serrano & Pérez-Fournon 1989, 1991, 1992).

The paper is organized as follows: in Sec. 2 we describe the sample of objects, observations, data reduction, and the surface photometry procedure used. In Sec. 3 a discussion

 0004-6256/93/051710-20$00.90 

of the individual objects is given. The general results on brightness profiles, absolute magnitudes, morphological peculiarities, and environment are presented in Sec. 4, and are compared with other samples of radio-loud and radio-quiet galaxies.

Throughout this paper $H_0=75$ km s$^{-1}$ Mpc$^{-1}$ and $q_0=0$ will be used. The visual absolute magnitudes, radio powers, and sizes taken from the literature have been converted to $H_0=75$ km s$^{-1}$ Mpc$^{-1}$. The radio powers were converted to the frequency of 1.4 GHz assuming a spectral index $\alpha=0.7$ ($S_\nu \propto \nu^{-\alpha}$) and are designated as $P_{eq}$.

## 2. OBSERVATIONS AND DATA REDUCTION

### 2.1 The Sample

The observed sample consists of 24 elliptical galaxies from the complete sample of low luminosity radio galaxies containing radio jets of Parma *et al.* (1987). These radio galaxies were originally selected for VLA observations from two lists of B2 sources associated with galaxies. The first sample contains B2 objects identified with galaxies in the *Zwicky Catalogue of Galaxies and Clusters of Galaxies* and is called the *bright* sample (Colla *et al.* 1975). The *faint* sample contains B2 radio sources identified with galaxies brighter than 17th mag on the Palomar Observatory Sky Survey plates (Fanti *et al.* 1978). The sources have radio power less than $10^{25}$ W Hz$^{-1}$ at 1.4 GHz and the redshifts are less than 0.15. Twenty-two radio galaxies have FR I morphology, one is of FR II class (0844+31) and the remaining one (1040+31) has undefined radio morphology. The observed galaxies are listed in Table I together with their radio properties.

TABLE 1. Radio galaxy sample.

| Name | $\alpha$ (1950) | $\delta$ (1950) | z | log$P^a_{1.4}$ W Hz$^{-1}$ | $L^b_{jet}$ kpc |
|---|---|---|---|---|---|
| 0034+25 | 00 34 26.8 | 25 25 26 | 0.0321 | 23.38 | 25 |
| 0206+35 | 02 06 39.3 | 35 33 41 | 0.0375 | 24.75 | 23 |
| 0836+29 | 08 36 13.4 | 29 01 17 | 0.0790 | 24.98 | 75 |
| 0836+29A | 08 36 59.1 | 29 59 45 | 0.0650 | 24.66 | 29 |
| 0844+31 | 08 44 54.1 | 31 58 12 | 0.0675 | 25.05 | 91 |
| 0908+37 | 09 08 45.4 | 37 36 33 | 0.1047 | 25.09 | 39 |
| 0915+32 | 09 15 56.8 | 32 03 52 | 0.0620 | 24.25 | 75 |
| 1040+31 | 10 40 31.0 | 31 46 45 | 0.0360 | 24.28 | 10 |
| 1243+26 | 12 43 54.6 | 26 43 39 | 0.0891 | 24.47 | 67 |
| 1254+27 | 12 54 59.4 | 27 46 02 | 0.0249 | 22.88 | 8 |
| 1322+36 | 13 22 35.4 | 36 38 19 | 0.0175 | 23.67 | 9 |
| 1357+28 | 13 57 45.2 | 28 44 28 | 0.0629 | 24.28 | 31 |
| 1450+28 | 14 50 23.8 | 28 10 15 | 0.1265 | 24.58 | 33 |
| 1521+28 | 15 21 21.4 | 28 48 07 | 0.0825 | 24.83 | 71 |
| 1525+29 | 15 25 40.5 | 29 06 15 | 0.0653 | 24.23 | 14 |
| 1528+29 | 15 28 05.9 | 29 10 43 | 0.0843 | 24.46 | 173 |
| 1553+24 | 15 53 56.8 | 24 35 31 | 0.0426 | 23.61 | 27 |
| 1637+29 | 16 37 22.2 | 29 56 47 | 0.0875 | 24.65 | 100 |
| 1643+27 | 16 43 26.6 | 27 25 30 | 0.1017 | 24.03 | 24 |
| 1658+30 | 16 58 48.9 | 30 12 32 | 0.0351 | 24.13 | 32 |
| 1736+32 | 17 36 45.2 | 32 57 36 | 0.0741 | 24.39 | 16 |
| 1827+32 | 18 27 04.9 | 32 17 59 | 0.0659 | 24.32 | 93 |
| 2116+26 | 21 16 20.7 | 26 14 08 | 0.0164 | 22.73 | 13 |
| 2236+35 | 22 36 12.3 | 35 04 11 | 0.0277 | 23.72 | 12 |

[a] Total radio power at 1.4 GHz from Parma et al. 1987

[b] Extension of the largest jet from Parma et al. 1987

### 2.2 Observations

The observations were carried out at the Observatorio del Roque de los Muchachos (La Palma, Spain). The CCD images were acquired during the four observing runs listed in Table 2. Observations on the Isaac Newton Telescope (INT) were made using GEC and RCA CCD cameras mounted at the prime focus. At the William Herschel Telescope (WHT) the observations were made using the TAURUS 2 $f/4$ focal reducer at the Cassegrain focus. We used the broad-band filters *B*, *V*, *R*, and *I* although not all the galaxies were observed in the four bands. The data were flux calibrated through observations of standard stars. The seeing was $\sim 1''$–$1''.3$ during the INT runs and about $1''.5$–$2''$ during the WHT run.

### 2.3 Data Reduction

The images were bias subtracted and flat-fielded using exposures of the twilight sky and of the dome illuminated by a lamp. The flat-field correction was found to be good to 0.5%. For the INT runs several exposures of the same object were taken in order to avoid excessive cosmic ray events, and guiding and saturation problems. These images were then co-added by measuring relative positions of field stars. For some objects the shift applied to several frames in the addition procedure was large and only the regions included in all the frames were analyzed. As a consequence, there are apparent empty regions in some of the contour maps shown here.

The sky background in each frame was calculated using three different methods: (1) average of the mean values in regions of the CCD images distant from the galaxy and free of interfering objects, (2) mode of the distribution of pixel intensities along the edge of the frame, and (3) the asymptotic value of the galaxy+sky intensity profile obtained from the isophote analysis procedure used. In most cases the three values agree to $\sim$0.3%. Once the sky level was determined, the data were calibrated to surface brightness in units of mag arcsec$^{-2}$ using observations of standard stars and corrected for galactic extinction (Burstein & Heiles 1982).

Figure 1 shows *V* band contour maps of 19 galaxies listed in Table 1 (except for B2 1637+29 which is an *R* band map). The remaining five objects (B2 0034+25, B2 0206+35, B2 0836+29, B2 2116+26, and B2 2236+35) have been discussed in González-Serrano & Pérez-Fournon (1991, 1992, hereafter Paper I and Paper II, respectively)

TABLE 2. Observing log.

| Date | Telescope | CCD | Scale (arcsec pixel$^{-1}$) | Field of view (arcmin×arcmin) | Comments |
|---|---|---|---|---|---|
| 1987 Oct | INT 2.5m | RCA | 0.74 | 6.3×3.9 | Photometric nights |
| 1988 Mar | WHT 4.2m | GEC | 0.27 | 1.7×2.6 | Photometric nights, poor seeing |
| 1989 Mar-Apr | INT 2.5m | GEC | 0.54 | 3.5×5.2 | Two non-photometric nights |
| 1990 June | INT 2.5m | GEC | 0.54 | 3.5×5.2 | Photometric night |

where contour maps, brightness profiles, and isophote parameters have been already presented. The sky surface brightness, noise in the sky, and lowest contour level for each map plotted in Fig. 1 are listed in Table 3.

### *2.4 Surface Photometry*

We have performed surface photometry of the galaxies by fitting ellipses to the isophotes. The procedure consists of a Fourier analysis of the intensity variations along elliptical contours fitted to the galaxy intensity distribution and is based on the GASP galaxy surface photometry package, written by Cawson (1983). A set of closely spaced elliptical contours is fitted to the intensity distribution of the galaxy. Free parameters are ellipticity, position angle, and ellipse center for every given semimajor axis. The intensity variations along the best-fit ellipse is expressed as a Fourier series including up to the fourth harmonic. The amplitude of the fourth cosine Fourier component relative to the mean intensity in the contour, the $B_4$ parameter, indicates deviations of the isophote shape from ellipticity in the form of "disky isophotes" ($B_4>0$) or "boxy isophotes" ($B_4<0$). A detailed discussion of the procedure and of the accuracy of the obtained parameters is given in Paper I.

We showed in that paper that the method is also useful to study galaxy pairs where one of the components dominates the total light distribution over a large area. There are several such systems in our sample and we have applied this method to those cases. A complicated system is the dumbbell galaxy B2 1450+28. In this case we applied iteratively the fitting procedure to both components until a flat residual was obtained. The isophote parameters and surface brightness profile must be, however, treated with caution, since the exact contribution to the common halo is not known. In the case of the galaxy B2 1736+32 the parameters can be affected by a bright star that contaminates the intensity distribution of the galaxy.

The surface brightness profiles obtained by the isophote analysis have been fitted by a de Vaucouleurs law. We restricted our linear regression fits to regions out of the nucleus ($r\gtrsim 2\farcs3$–$3''$) to minimize the effects of seeing. The outer radius of the fitting region was that for which the photometric errors started to be significant ($\sim$0.3 mag) or the profile began to deviate from the $r^{1/4}$ law, due to the presence of an envelope, shells, etc. The effective surface brightness ($\mu_e$) and radii ($r_e$) obtained from the best fit are listed in Table 4.

## 3. INDIVIDUAL GALAXIES

In Fig. 2 we present the resulting surface brightness profiles and isophote parameters obtained from the ellipse fitting algorithm. The profiles correspond to the $V$ band except for B2 1637+29 which correspond to the $R$ filter. The isophote parameters are affected by the seeing and therefore they are not reliable in the inner part of the galaxies.

In this section we briefly discuss some properties of the 24 galaxies in the sample inferred from the optical data. Comments are also made on the 1.4 GHz radio jets, whose maps can be found in Parma *et al.* (1986), de Ruiter *et al.* (1986), and Fanti *et al.* (1986).

**0034+25.** This radio galaxy shows a wide angle tail morphology with an inner double jet in P.A. 90°. It has a nearby companion located at a projected distance of 26 kpc and it shows indications of gravitational interaction (Paper I). The galaxy has an inner stellar disk perpendicular to the radio jet and that has been interpreted as the signature of a past merging (González-Serrano & Pérez-Fournon 1989).

**0206+35.** This source shows a double jet in the NW–SE direction. The galaxy is located in the Zwicky cluster 0216.0+3625 and has a close companion at a projected distance of 31 kpc in P.A. 110°. The main galaxy shows strong isophote distortions, suggesting the presence of a tidal tail, and also exhibits indications of a dust lane in the core. A detailed photometric analysis shows that both galaxies are interacting (Paper I).

**0836+29.** This is the brightest member in the cluster Abell 690. It presents two lobes and an inner one-sided jet in P.A. 0°. The galaxy has an associated x-ray halo with a size comparable to that of the radio emission (Morganti *et al.* 1988). From our photometric analysis we found an extended envelope in the external parts of the galaxy and concluded that 0836+29 is a multiple nuclei cD galaxy (Paper II).

**0836+29A (4C29.30).** A detailed radio and optical study of this radio source has been made by van Breugel *et al.* (1986) who present VLA, optical imaging, and spectroscopic observations. The authors found extended optical line emission adjacent to the radio jet (in P.A.$\sim$20°) and they present evidence that the radio jets are interacting with dense extranuclear gas. On the basis of the presence of shells and dust, the authors suggested that 4C29.30 is the

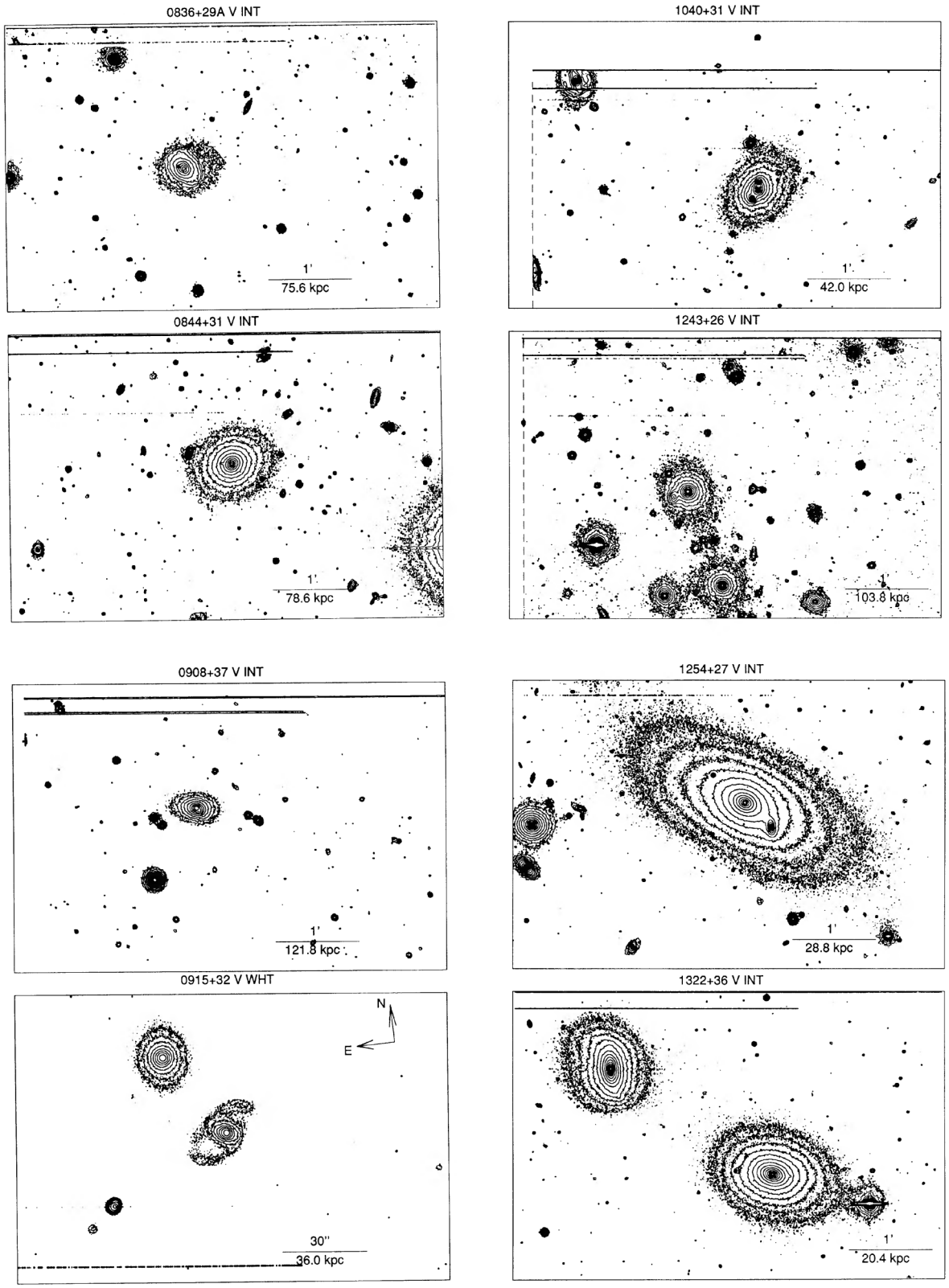


FIG. 1. Contour maps of the observed galaxies. All maps are *V* band images except B2 1637+29 which is an *R* band frame. Unless indicated on the map, North is up and East is to the left. First contours are given in Table 3, being the interval between consecutive contours of 0.5 mag. Empty regions that appear in some of the maps (delimited by dashed lines) arose from large positional offsets in the addition procedure.

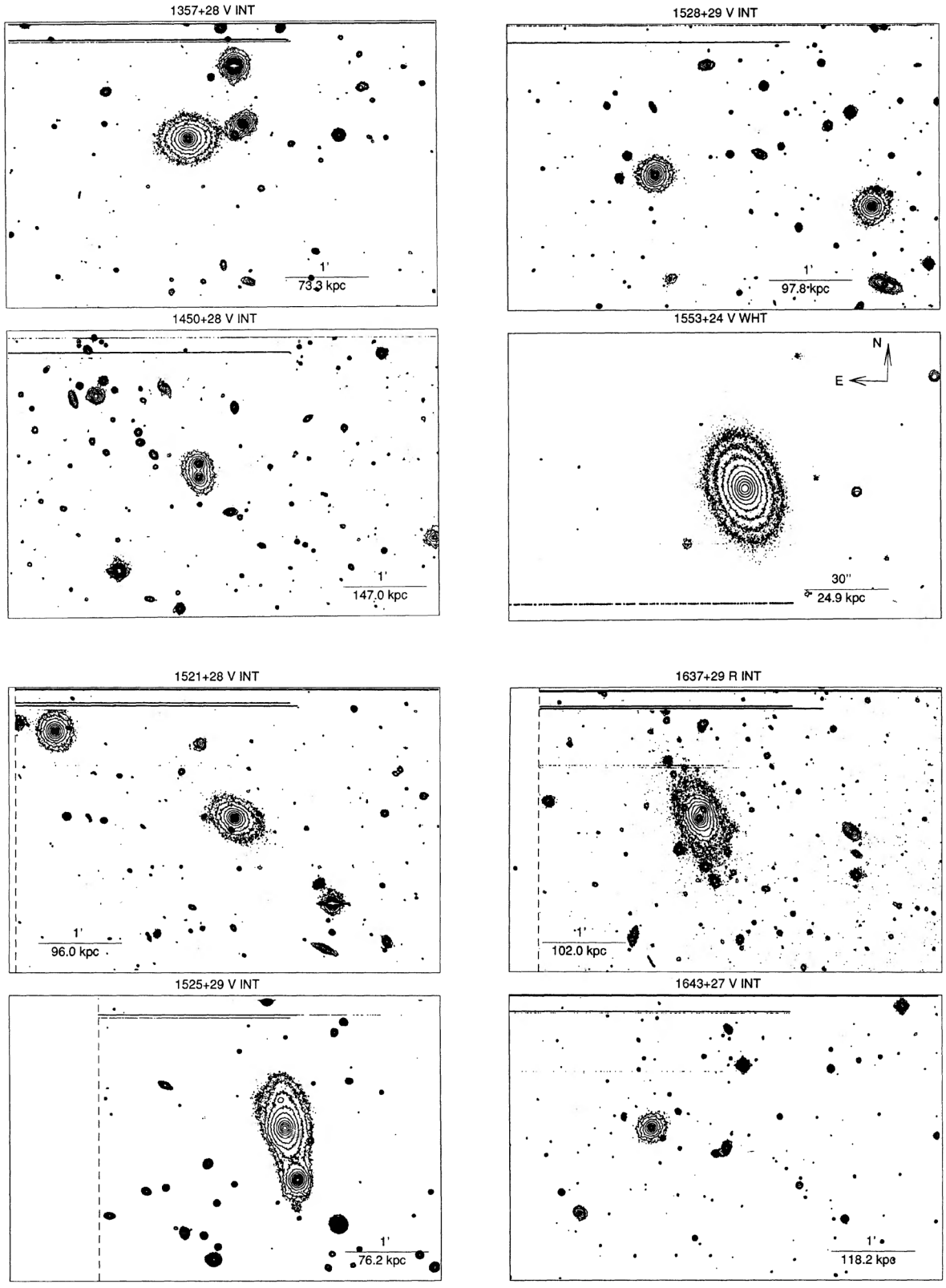


FIG. 1. (continued)

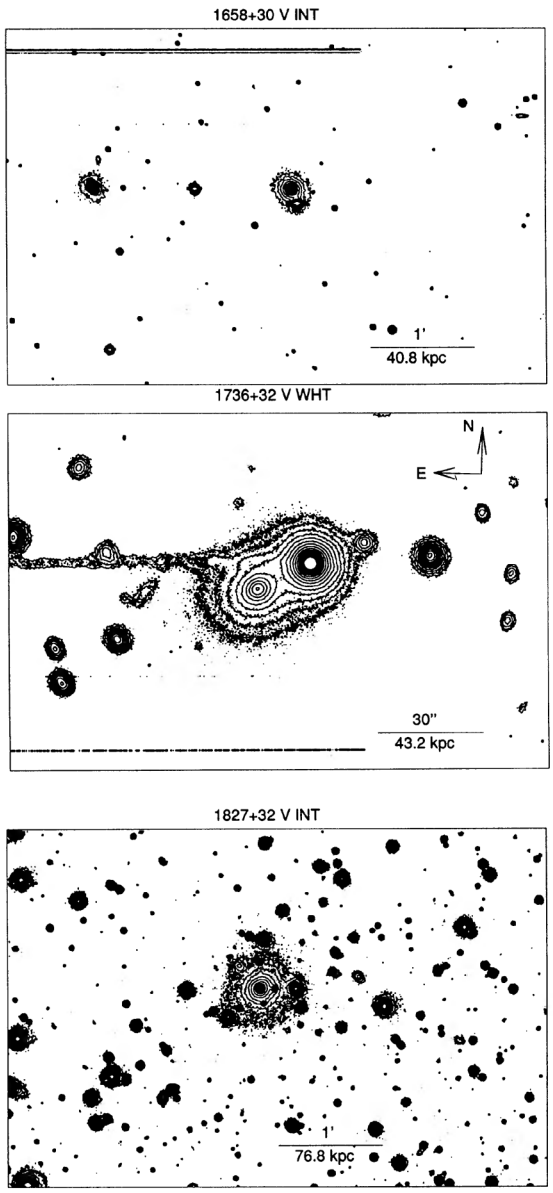


FIG. 1. (continued)

result of a merger with a gas-rich galaxy. These features are observed in our $V$ image. The dust lane is visible in the nuclear region and is producing high $B_4$ values and changes in ellipticity and in the major axis position angle (see Fig. 2). The outer shell and the emission line regions detected by van Breugel *et al.* (1986) are also clearly visible in the $V$ frame. A sharp edge is observed in the outer parts of the galaxy, at the NE side. The sharp edge and the shells are also revealed in the surface brightness profile which, on the other hand, fits well to an $r^{1/4}$ law in the central regions.

**0844+31 (4C31.32).** This galaxy is one of the most powerful radio galaxies of the sample and presents a FR II morphology with two lobes located at ~90 kpc from the core. Our CCD data reveal an elliptical galaxy with no isophotal distortions and with a brightness profile following the $r^{1/4}$ law. A smooth isophote twisting of ~30° from the nucleus to the external parts is present. The galaxy belongs to a Zwicky cluster and Morganti *et al.* (1988) report an unresolved x-ray source associated with the radio galaxy.

TABLE 3. Sky, noise, and 1st contour levels.

| Galaxy | Run | $\mu$(sky) | $\mu$(noise) | $\mu$(1st) |
|---|---|---|---|---|
| 0836+29A | 3 | 21.5 | 26.2 | 25.2 |
| 0844+31 | 3 | 21.2 | 25.9 | 24.4 |
| 0908+37 | 3 | 21.5 | 26.1 | 24.6 |
| 0915+32 | 2 | 21.1 | 24.5 | 23.0 |
| 1040+31 | 3 | 21.3 | 26.0 | 24.5 |
| 1243+26 | 3 | 20.9 | 25.8 | 24.3 |
| 1254+27 | 3 | 21.3 | 25.7 | 24.8 |
| 1322+36 | 3 | 21.2 | 25.7 | 24.2 |
| 1357+28 | 3 | 21.1 | 25.8 | 24.3 |
| 1450+28 | 3 | 20.7 | 25.7 | 24.2 |
| 1521+28 | 3 | 20.8 | 25.8 | 24.3 |
| 1525+29 | 3 | 21.0 | 25.7 | 24.2 |
| 1528+29 | 3 | 21.7 | 26.3 | 24.8 |
| 1553+24 | 2 | 21.7 | 24.8 | 23.3 |
| 1637+29[a] | 3 | 20.5 | 25.3 | 24.2 |
| 1643+27 | 3 | 20.3 | 25.4 | 23.9 |
| 1658+30 | 3 | 19.8 | 24.8 | 23.3 |
| 1736+32 | 2 | 21.7 | 24.8 | 23.3 |
| 1827+32 | 4 | 21.7 | 26.2 | 24.7 |

[a] R magnitudes

**0908+37.** This is the most powerful radio source of the sample and presents a jet in P.A. 14° and two lobes in an extended diffuse emission. The object is associated with a flat galaxy (ellipticity ~0.3–0.4) which follows the $r^{1/4}$ law. Our CCD image shows a compact object near the nucleus, which is most probably a faint star.

**0915+32.** The radio map by Fanti *et al.* (1987) presents a two-sided jet in P.A. 28° with mirror symmetry. The jets bend at ~40″ from the core and the morphology is remarkably similar to that of 3C31 (Blandford & Icke 1978). The poor seeing has smoothed out our CCD image. It shows a normal elliptical with a nearby spiral galaxy at a projected distance of 35″ (42 kpc) in P.A. 219°. As Parma *et al.* (1985) suggested, the jet distortions could be explained by the interaction between the two galaxies. Unresolved nuclear H$\alpha$+[N II] emission has been detected by Morganti *et al.* (1992).

TABLE 4. Photometric parameters.

| Name | $\mu_e$ | ± | $r_e$ (arcsec) | ± | $r_e$ (kpc) | ± |
|---|---|---|---|---|---|---|
| 0034+25 | 23.04 | 0.040 | 42.57 | 0.64 | 26.50 | 0.40 |
| 0836+29 | 22.41 | 0.030 | 8.09 | 0.13 | 12.40 | 0.20 |
| 0836+29A | 25.09 | 0.056 | 31.86 | 1.34 | 40.13 | 1.69 |
| 0844+31 | 22.69 | 0.032 | 13.17 | 0.25 | 17.23 | 0.33 |
| 0908+37 | 23.79 | 0.046 | 12.41 | 0.36 | 25.18 | 0.73 |
| 0915+32 | 21.66 | 0.093 | 4.64 | 0.24 | 5.57 | 0.29 |
| 1040+31 | 22.64 | 0.047 | 9.23 | 0.27 | 6.44 | 0.19 |
| 1243+26 | 21.57 | 0.041 | 4.64 | 0.10 | 8.02 | 0.17 |
| 1254+27 | 22.63 | 0.029 | 26.33 | 0.57 | 12.70 | 0.27 |
| 1322+36 | 20.90 | 0.023 | 10.09 | 0.13 | 3.42 | 0.04 |
| 1357+28 | 22.25 | 0.049 | 6.54 | 0.18 | 7.97 | 0.22 |
| 1450+28 | 22.84 | 0.130 | 5.60 | 0.40 | 13.73 | 0.98 |
| 1521+28 | 22.42 | 0.055 | 6.28 | 0.20 | 10.04 | 0.32 |
| 1525+29 | 21.35 | 0.047 | 4.09 | 0.10 | 5.18 | 0.12 |
| 1528+29 | 22.21 | 0.059 | 5.97 | 0.21 | 9.75 | 0.34 |
| 1553+24 | 22.55 | 0.063 | 11.45 | 0.44 | 9.45 | 0.36 |
| 1637+29 | 22.71 | 0.077 | 12.80 | 0.65 | 21.70 | 1.10 |
| 1643+27 | 23.69 | 0.043 | 9.60 | 0.27 | 18.92 | 0.53 |
| 1658+30 | 20.79 | 0.052 | 3.33 | 0.08 | 2.26 | 0.05 |
| 1736+32 | 23.22 | 0.088 | 15.46 | 1.03 | 22.20 | 1.48 |
| 1827+32 | 22.93 | 0.027 | 8.95 | 0.15 | 11.43 | 0.19 |
| 2116+26 | 21.87 | 0.040 | 23.50 | 0.40 | 7.47 | 0.13 |
| 2236+35 | 22.58 | 0.020 | 24.29 | 0.30 | 13.05 | 0.16 |

**1040+31.** Our image shows an elliptical galaxy with an aligned triple nucleus. The brightness profile presents an extended outer envelope. Most probably this object can be classified as a cD galaxy. Two bright galaxies are seen in the field, as well as some other faint galaxies. The radio morphology is quite peculiar (see the 1.4 GHz map in Fanti *et al.* 1986). It shows an extended halo with a jet connecting the core with a hot spot in P.A. 162°, roughly aligned with the three central components. Morganti *et al.* (1992) report unresolved nuclear H$\alpha$ emission.

**1243+26.** This radio source is located in the cluster Abell 1609. In the VLA map by Fanti *et al.* (1987) the radio source appears to be composed of two radio galaxies separated by 1'.20 along P.A. 200°. The Northern source presents a two-sided jet emerging to the NE and SW directions, and shows well resolved sharp bends at a projected distance of about 50 kpc from the core. At larger distances the jets expand. The Southern component shows extended emission at a very low surface brightness level and with a low degree of collimation.

The elliptical galaxy located near the center of our *V* frame is the optical counterpart of the Northern radio source. The position of the Southern radio source coincides, within 0".18, with another bright elliptical. The surface brightness profile and isophote parameters shown in Fig. 2 correspond to the Northern galaxy.

Several facts suggest that both galaxies are interacting: (1) the morphology of the radio jets shows mirror symmetry recalling the case of 3C31 (Blandford & Icke 1978); (2) the abrupt change in P.A. of the brightest galaxy from $\sim$90° in the inner parts to $\sim$20° (i.e., in the direction of the companion) in the outer isophotes; (3) the presence of a faint bridge of emission linking both galaxies. The brightness profile shows an excess over the de Vaucouleurs law that fits the inner parts.

**1254+26 (NGC 4839).** This is a bright cD galaxy in the Coma cluster, although not located at its center (Davies & Illingworth 1983). Our brightness profile shows the extended envelope, consistent with that observed by Schombert (1986). Significant boxy isophotes are present (see Fig. 2). A relatively faint galaxy is located at 12.3 kpc (25".6) in P.A. 227°. A two-sided radio jet with slight distortions emerges in P.A. $\sim$0°. Unresolved nuclear H$\alpha$ emission has been detected by Morganti *et al.* (1992).

**1322+36 (NGC 5141, 4C36.24).** The *V* image shows two bright galaxies separated by 2'.3 (47 kpc), the Southwestern one containing the radio source. The NE companion, NGC 5142, is clearly distorted and shows boxy and disklike isophotes. The radial velocities of the galaxies differ only by 53 km s$^{-1}$ (Soares 1989). The radio source presents a two-sided jet in P.A. 12°, although both jets bend by $\sim$45°, showing S symmetry.

The brightness profile is well represented by an $r^{1/4}$ law and the isophotes are nonelliptical in shape. Positive ($r \lesssim 10''$) and negative ($r \gtrsim 10''$) $B_4$ isophotes are present (see Fig. 2). NGC 5141 is a clear example of an interacting galaxy with distorted jet morphology. Emission in the H$\alpha$ line has been observed in the nuclear region (Morganti *et al.* 1992).

**1357+28.** Elliptical galaxy with an extended envelope in the outer parts and with undisturbed isophotes. It has two small galaxies at 50 kpc (41".2) in P.A. $\sim$285° and some other faint galaxies are seen in the field. The radio map of Fanti *et al.* (1987) shows a two-sided inner jet in P.A. 0.5° that decollimates and bends at 30" from the core. The radio emission has mirror symmetry, suggesting gravitational interaction.

**1450+28.** Dumbbell system in the center of the cluster Abell 1984. The radio galaxy is associated with the southern galaxy of the pair and shows a slightly bent jet roughly perpendicular to the line, in P.A. 0°, connecting both galaxies. Valentijn & Casertano (1988) measured a relative radial velocity of 1000 km s$^{-1}$ between both nuclei.

After several iterations in order to mask out the northern galaxy, we were able to obtain a reliable fit for the southern galaxy, which shows no distortions and a brightness profile well reproduced by a de Vaucouleurs law.

**1521+28.** This galaxy has a brightness profile showing excesses over the de Vaucouleurs law in the external parts. Several small galaxies and an elliptical located at 230 kpc (2'.4) in P.A. 64° appear in the field. The radio source has an inner ($\lesssim 15''$) jet in P.A. 149° that bends showing S symmetry.

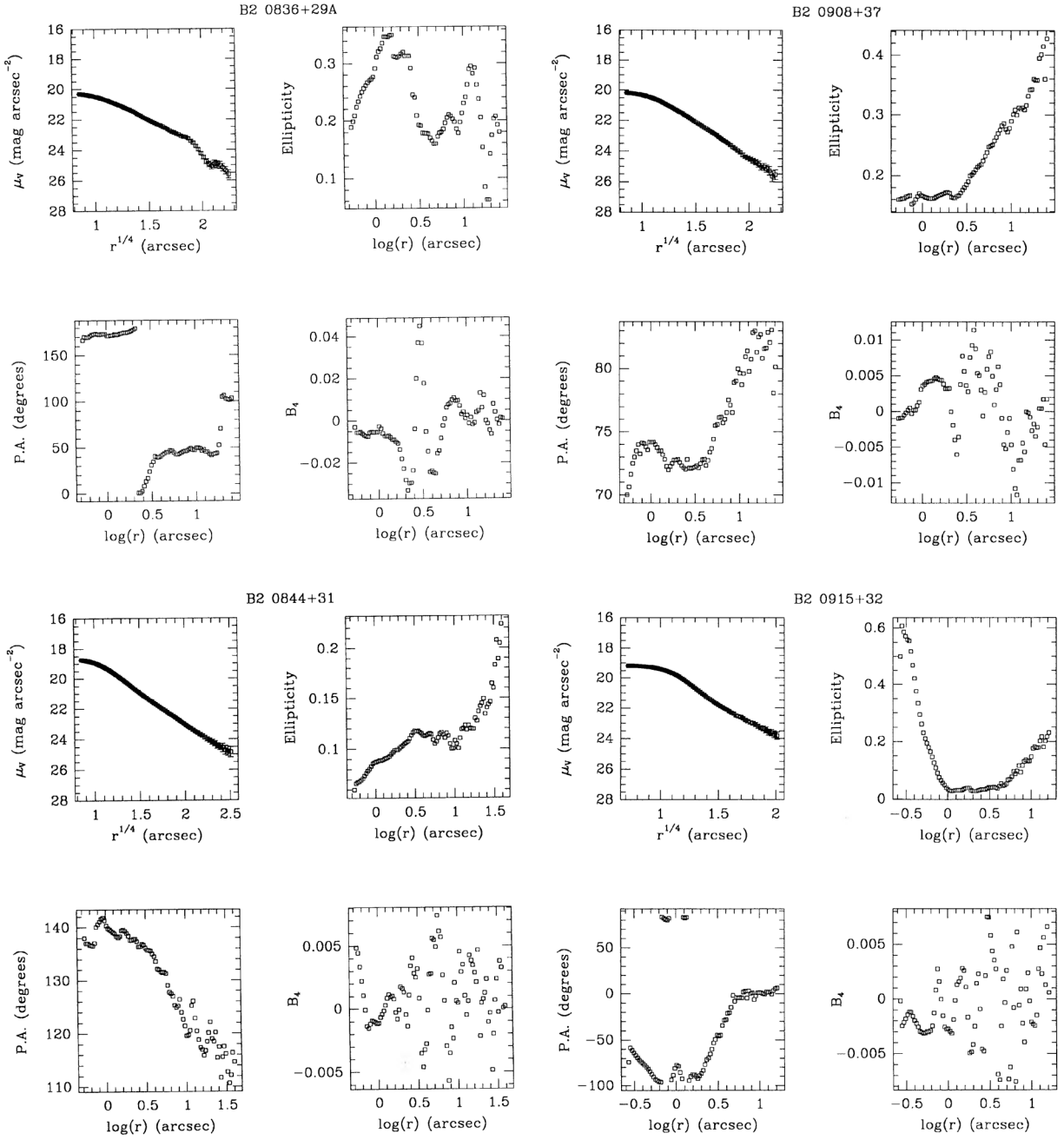


FIG. 2. The $V$ band surface brightness, ellipticity, semimajor axis, position angle, and $B_4$ profiles for the observed galaxies. The data for B2 1637+27 correspond to $R$ band.

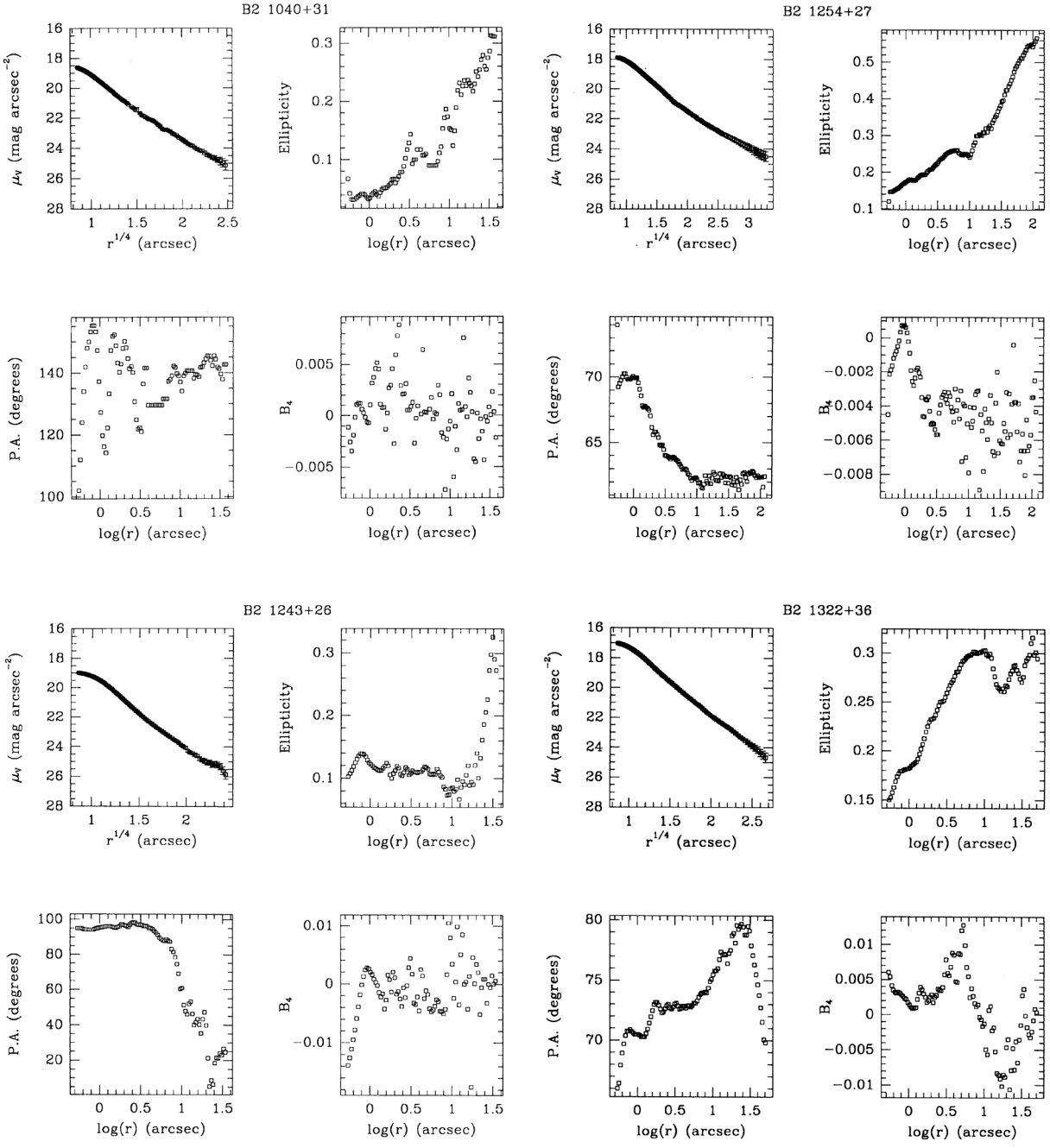


FIG. 2. (continued)

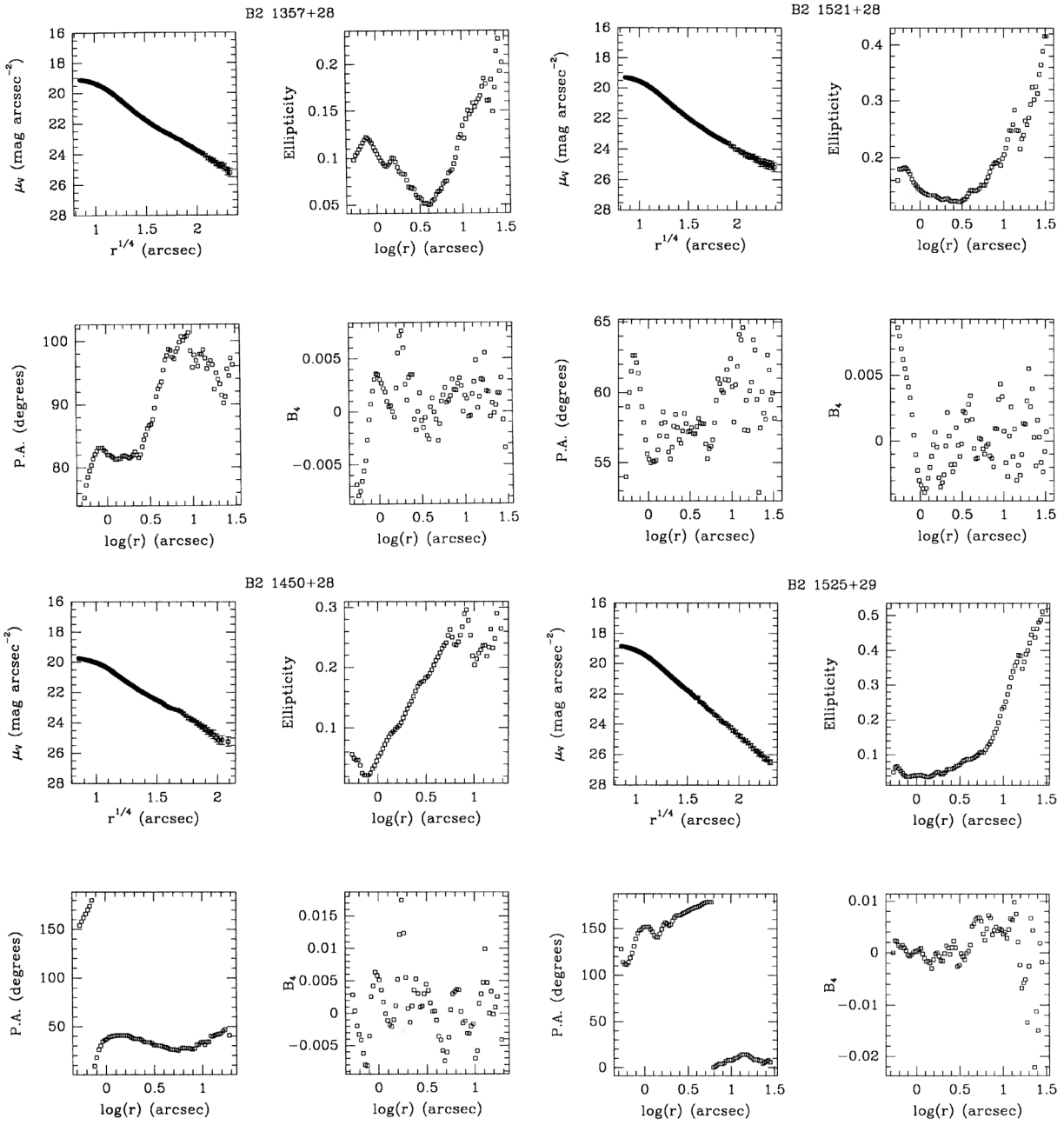


FIG. 2. (continued)

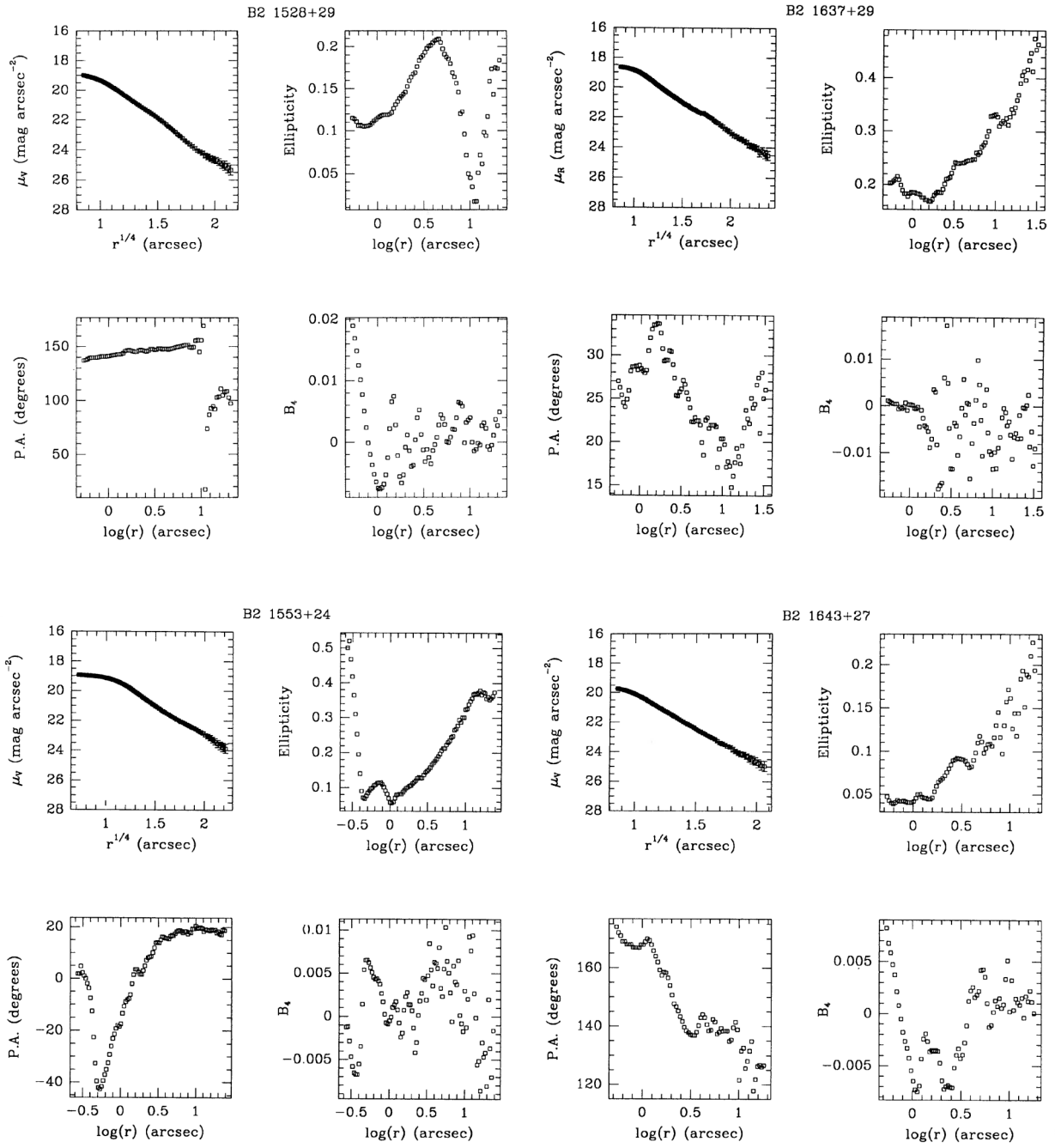


FIG. 2. (continued)

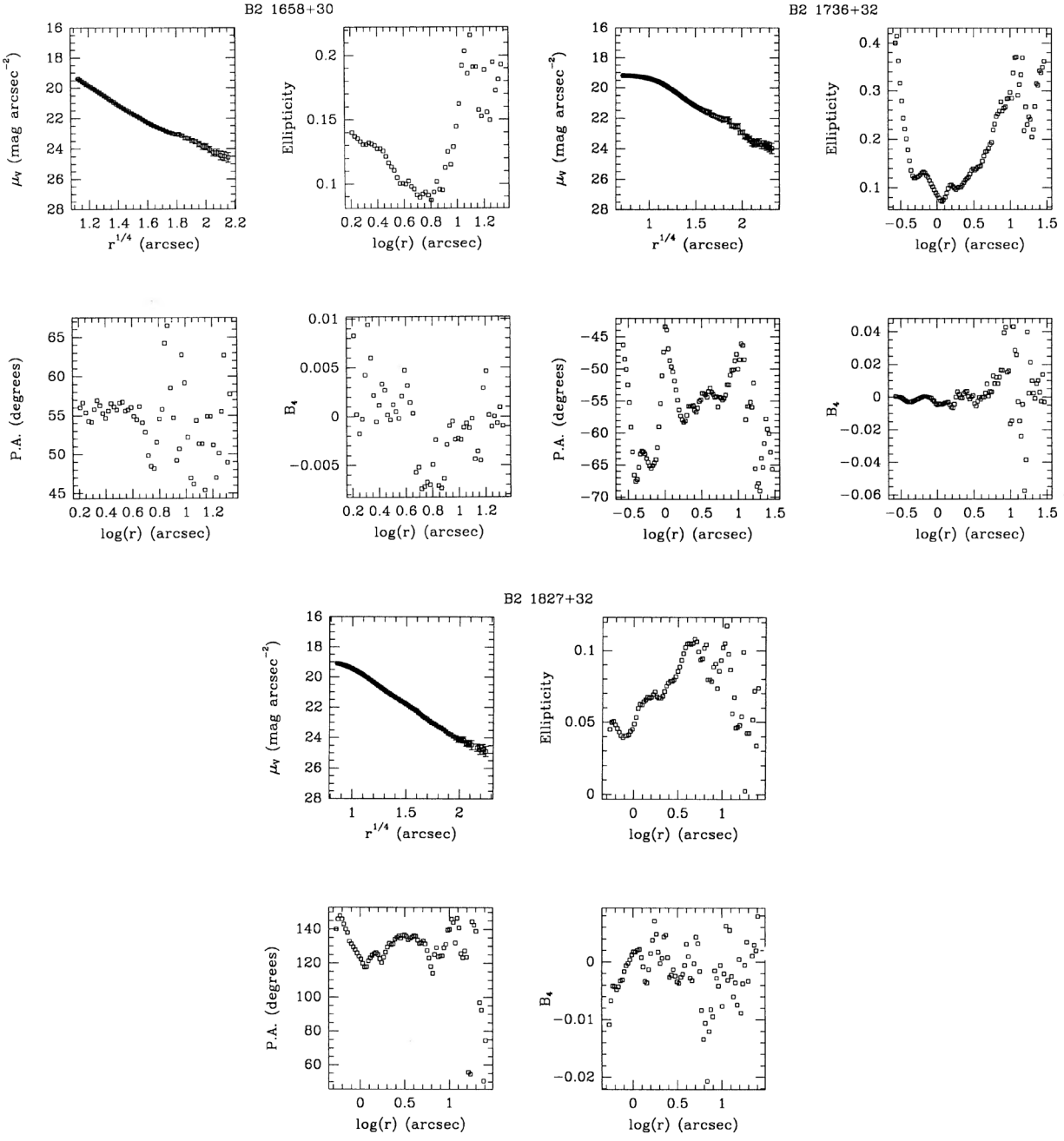


FIG. 2. (continued)

**1525+29.** The $V$ image shows a dumbbell system in which the Southern and smaller galaxy is the radio source. There is evidence of another faint galaxy North of the main component. The group is located at the center of the cluster Abell 2079 (Fanti *et al.* 1983). This system was observed by Valentijn & Casertano (1988) who measured a relative velocity of 20 km $s^{-1}$ between both galaxies. The optical counterpart of the radio galaxy has a de Vaucouleurs profile and disklike isophotes in the outer regions. The brightest galaxy, separated by 39".2 (50 kpc), is very highly distorted, showing also disklike isophotes in the outer parts.

The two-sided radio jet is also distorted. Extended x-ray emission is present, although at a larger scale than the radio emission (Morganti *et al.* 1988).

**1528+29.** Elliptical galaxy located in a rich environment with a nearby galaxy of similar luminosity at 2'.6 (255 kpc) in P.A. 262°. The radio emission presents a two-sided jet in P.A. 57° that ends in two lobes slightly distorted. The surface brightness profile fits well a de Vaucouleurs law. In the inner 10" the galaxy is flatter than in the outer regions, and the major axes of the isophotes show a correlated twisting with changes in ellipticity (see the $V$ map in Fig. 1 and the parameter profiles in Fig. 2).

**1553+24.** The radio source, which is characterized by a double jet without lobes, has been studied in detail by Morganti *et al.* (1987). Note in Fig. 2 how the isophote parameters in the inner parts are affected by the bad seeing. The galaxy has some excesses over the $r^{1/4}$ law in the outer parts. Morganti *et al.* (1988) detected weak x-ray emission and, more recently, unresolved nuclear H$\alpha$ emission (Morganti *et al.* 1992).

**1637+29.** VLA observations of this radio source presented by de Ruiter *et al.* (1988) show a very distorted radio tail which curves back strongly. These authors conclude that the galaxy could be the dominant member of a galaxy-poor cluster, and explain the unusual radio morphology as a result of the physical encounter with a nearby galaxy and the nonuniform motion of the radio source with respect to the intergalactic medium. Although the relative velocity of this nearby galaxy is high (4300 km $s^{-1}$), de Ruiter *et al.* argue that a chance superposition is highly improbable and that the undulation observed in the radio emission can only be caused by a very high velocity encounter between two galaxies.

Our $R$ map, with better seeing and signal-to-noise ratio than the one shown by de Ruiter *et al.* (1988), shows a bright elliptical with a nearby compact object to the northwest which is the companion interacting with the radio galaxy at a relative velocity of 4300 km $s^{-1}$. At low surface brightness levels some emission is detected in the outer parts of the main galaxy, most probably being shells resulting from the encounter. The $B_4$ profile could reflect some boxiness in the isophotes, although the profile is rather noisy.

**1643+27.** Small and round galaxy that follows the $r^{1/4}$ law. It shows boxy isophotes in the inner parts ($r \lesssim 4''$) albeit at a low level. We note however, that this could be affected by poor seeing or bad tracking. The radio jet is in P.A. 12° and shows two lobes and some knotty structure. The inner jet extends over 24 kpc and the lobes are located 120 kpc from the core.

**1658+30 (4C30.31).** The source is a 32 kpc one-sided jet embedded in a diffuse emission. The jet is in P.A. 232° and ends in a hot spot. The CCD image shows an elliptical with a nearby galaxy at 1'.91 (78 kpc) in P.A. 89°. The galaxy follows the de Vaucouleurs law in the inner parts but shows excesses in the outer parts.

**1736+32.** This source has a remarkable radio structure that has been interpreted as superimposition of two unrelated sources (Fanti *et al.* 1986). Our $V$ image shows an elliptical galaxy with a bright (saturated) star to the NW and other faint galaxies in the field. The horizontal band crossing the frame is an instrumental artifact caused by charge leakage from the saturated star. The isophotal parameters are affected by the presence of the saturated star in the external parts.

**1827+32.** The radio map by de Ruiter *et al.* (1986) shows an inner two-sided jet in P.A. 72° and two diffuse components. There is a change in P.A. of $\sim$60° from the core to the outer SW component. The overall morphology suggest a precession phenomenon of the central engine. The optical counterpart of the radio source is an elliptical with a brightness profile following a de Vaucouleurs law and it is located in a region with a few fainter galaxies. A low surface magnitude object, most probably a galaxy, is detected at 18" (23 kpc) in P.A. 42°.

**2116+26 (NGC 7052).** The VLA map of the source shows a two-sided jet with a total length of 26.6 kpc in P.A. 21° and 201°. Our $V$ image reveals a bright galaxy with external ($r \gtrsim 28''$) boxy isophotes and inner positive $B_4$ terms. This galaxy presents a small dust lane in the core that could be the result of a past merging process (Paper II).

**2236+35.** This source is located in the Zwicky cluster 2231.2+3732. It has a two-sided radio jet embedded in a distorted low-brightness region with $S$ symmetry. Several bright galaxies are found on the $V$ image. The photometric analysis of the optical counterpart of the radio source and two nearby ellipticals in the field suggests a gravitational encounter (Paper II).

## 4. GENERAL RESULTS AND DISCUSSION

In this section the results obtained from our optical imaging of low power radio sources are discussed and compared with those found in the literature for powerful and radio-quiet galaxies.

### *4.1 Galaxy Photometry*

#### *4.1.1 $\mu_e$ vs $r_e$*

In Fig. 3(a) we have represented the de Vaucouleurs parameters $\mu_e$ and $r_e$ obtained from the fits to the surface brightness profiles of the galaxies of the sample, along with the best fit line:

$$\mu_e(V \text{ mag arcsec}^{-2}) = 19.42 \pm 0.31 + (3.00 \pm 0.29)\log [r_e(\text{kpc})].$$

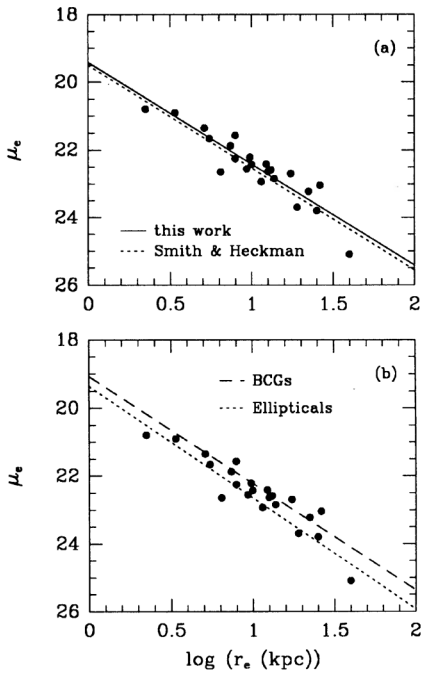


FIG. 3. Surface brightness ($\mu_e$) vs effective radius ($r_e$) for the galaxy sample. The lines on the top panel (a) show the best linear regression fit for this sample and that for the sample of galaxies by SH ($P_{eq} > 10^{24.3}$ W Hz$^{-1}$). The lines on the bottom panel (b) show the best linear regressions for normal ellipticals (Kormendy 1980) and Bright Cluster Galaxies (BCG; Hoessel *et al.* 1987).

The fit is practically identical to that found by Smith & Heckman (1989b, hereafter SH) for a larger sample of 72 intermediate and powerful radio sources with $P_{eq} \gtrsim 10^{24.3}$ W Hz$^{-1}$. The SH fit, shown by the dashed line in Fig. 3(a), is

$$\mu_e(V \text{ mag arcsec}^{-2}) = 19.50 \pm 0.30 + (3.03 \pm 0.29) \log [r_e(\text{kpc})].$$

Figure 3(b) shows that, as it occurs for the radio galaxies in the SH sample, the radio galaxies in our study fall, as a whole, between normal elliptical galaxies (Kormendy 1980) and bright cluster galaxies (BCG, Hoessel *et al.* 1987), which respectively follow the laws:

$$\mu_e(V \text{ mag arcsec}^{-2}) = 19.36 + 3.28 \log[r_e(\text{kpc})]$$

(normal ellipticals)

$$\mu_e(V \text{ mag arcsec}^{-2}) = 19.08 \pm 0.13 + (3.14 \pm 0.09) \times \log [r_e(\text{kpc})] \quad \text{(BCG)}.$$

The dispersion of the data around the fitted lines, and the range in $\mu_e$ and $r_e$ are similar for the four samples.

#### *4.1.2 Isophotal properties*

In this section we summarize the morphological peculiarities found in our sample of galaxies. A list of the galaxies that exhibit significant departures from elliptical symmetry in their optical morphology is given in Table 5. The peculiarities include the presence of boxy and disky isophotes, isophote twisting, shells, bridges, extended envelopes, and dust.

TABLE 5. Optical morphology.

| Galaxy | Feature | Galaxy | Feature |
|---|---|---|---|
| 0034+26 | DI, TI | 1521+28 | Ex |
| 0206+35 | D, TI | 1525+29 | DI |
| 0836+29 | Ex | 1528+29 | TI |
| 0836+29A | D, S | 1553+24 | Ex |
| 0844+31 | TI | 1637+29 | BI?, S |
| 1040+31 | Ex | 1643+27 | BI? |
| 1243+26 | B, Ex, TI | 1658+30 | Ex |
| 1254+27 | BI, Ex | 2116+26 | BI, D, DI |
| 1322+36 | BI, DI | 2236+35 | TI |
| 1357+28 | Ex | | |

Key of features:
B: bridge
BI: boxy isophotes
D: dust lane
DI: disky isophotes
Ex: excesses over the de Vaucouleurs law
S: shells
TI: twisting of isophotes

Six galaxies of the sample (25%) have high isophote twisting ($\gtrsim 20°$ per decade in semimajor axis), occurring in four cases in the direction of a close neighbor. Eight objects (33%), including the three cD galaxies, have surface brightness profiles which show excesses over the $r^{1/4}$ law that fits the inner parts of the galaxy. Three galaxies (12%) show faint shells or bridges connecting to a companion and another one (B2 0206+35) shows highly distorted inner isophotes with a high $B_3$ component, that could be associated with the presence of a tidal tail. Three galaxies (12%) have small dust lanes in their cores and 17% (four galaxies) have central ($\lesssim 10''$) disky isophotes. Three galaxies in our sample (12%) have significant boxy isophotes. Two others present some evidences of boxy isophotes but their $B_4$ profiles are rather noisy to clearly classify them as galaxies with boxy isophotes.

Considering shells, bridges, dust, disks, boxiness, isophote twisting, and extended outer envelopes, 18 out of 24 galaxies, i.e., 75% of the sample, present one or several of these peculiarities.

Systematic studies of isophote shapes in ellipticals have led to the discovery of a strong correlation between radio emission and boxy isophotes (Bender *et al.* 1987, 1989). Nieto & Bender (1989) suggested that boxiness is likely to be originated in merging processes or gravitational inter-

actions. The three galaxies in our sample presenting boxy isophotes have additional indicators of merging or interaction. B2 1322+36 (NGC 5141) has a distorted jet morphology in the radio and is paired with NGC 5142, B2 2116+26 presents a nuclear dust lane most probably formed in a merger event, and B2 1254+27 is a cD galaxy likely the result of mergers and cannibalism. Also B2 1637 +29, with possible boxy isophotes, seems to be undergoing an interaction event.

Our analysis seems to suggest that radio emission does not necessarily imply boxy isophotes. This appears to be in contradiction with Bender *et al.* (1987) who claim a strong correlation between boxiness and radio emission in elliptical galaxies. By reanalyzing this relation, Bender *et al.* (1989) conclude that radio emission (and x-ray halos) occurs predominantly in elliptical galaxies with *boxy* or *irregular isophote shapes,* which is more consistent with our results. We found a low fraction of disky ellipticals also in agreement with Bender *et al.* (1989).

#### *4.1.3 Absolute magnitudes*

We have measured the $V$ magnitudes of the galaxies using a simple aperture scheme. We selected apertures whose radii were equal to, or slightly larger than, the radius where the intensity gradient reached zero. Stars, galaxies or "additional nuclei" (with luminosities substantially less than that of the main body of the galaxy, to distinguish from double systems with two components of approximately equal luminosities) within the outline of the galaxies were removed, substituting their counts by the mean intensity value in adjacent positions. The apparent $V$ magnitudes, absolute $V$ magnitudes, and aperture sizes used for the galaxies in this work are listed in Table 6. We have applied the $K$-correction from Bruzual (1983) to obtain the absolute visual magnitude.

The absolute magnitudes of the galaxies in our sample can be compared with the values obtained by SH for their completely independent sample of 72 radio galaxies with $\log P_{\rm eq} > 24.3$. Although the SH magnitudes have been corrected for nonstellar continuum and emission-line gas, our magnitudes can be considered as intrinsic since, given the known relation between line strength and radio luminosity (Hine & Longair 1979; Baum & Heckman 1989a,b; Morganti *et al.* 1992), the corrections for our galaxies are expected to be low.

The mean absolute magnitude of our sample is $\langle M_V \rangle = -22.37$ with a dispersion of $\sigma = 0.58$, in perfect agreement with that obtained by SH for the 31 galaxies with weak or no emission lines (WE/ABS) in their sample, $\langle M_V \rangle = -22.39$ ($\sigma = 0.67$). The mean absolute magnitude of the 41 strong optical emission lines (SE) objects in the SH sample is $\langle M_V \rangle = -22.04 (\sigma = 0.64)$, which is consistent with that obtained for their 51 PRG with $\log P_{\rm eq} > 25$, $\langle M_V \rangle = -22.11$ ($\sigma = 0.66$). The SE galaxies are therefore 0.33 magnitudes fainter than the LLRG with radio jets in our sample (difference significant at the 96% confidence level). We thus confirm the previous result that the host galaxies of LLRG with radio jets are *intrinsically* brighter than those associated with PRG with strong emission lines (Lilly & Prestage 1987; Owen & Laing 1989). As a matter of fact, Lilly & Prestage (1987) and Owen & Laing (1989) had found a relation between *Fanaroff–Riley class and absolute magnitude,* in the sense that FR I radio galaxies (usually of low radio power) are optically more luminous than FR II radio galaxies (usually of high radio power).

Lilly & Prestage (1987) and SH remarked the similarity between the absolute magnitudes of FR I–WE/ABS radio galaxies and bright cluster galaxies, with $\langle M_V \rangle = -22.37$ and $\sigma = 0.32$ (Sandage 1972). The data on our sample of LLRG clearly confirm this result. The trend in the sense of a decrease in the luminosity of the host galaxy as a function of radio power could be related to a higher extinction in PRG due to the presence of larger amounts of dust (H86). Another possibility is that LLRG with radio jets and PRG are intrinsically different kinds of galaxies (H86; Lilly & Prestage 1987; Owen & Laing 1989).

### *4.2 Local Galaxy Density*

In recent years there has been growing interest in the study of the environment of radio sources. In order to quantify the local galaxy density of the galaxies in our sample we have measured the parameters $\rho_{00}$, $\rho_{01}$, $\rho_{10}$, and $\rho_{11}$ as defined by Heckman *et al.* (1985, hereafter HCB). These parameters describing the local galaxy density are related to the local gravitational interaction suffered by the radio galaxy, with $\rho_{00}$ giving the number of galaxies, $\rho_{01}$ accounting for the sizes of the neighbors, $\rho_{10}$ weighting the companion galaxies according to their proximity to the radio source, and $\rho_{11}$ weighting them according to both relative size and proximity (see HCB for details). We want to note that large values of $\rho_{01}$ and $\rho_{11}$ can arise from both, a large numerical density of galaxies (what we can call "clustering") and the presence of a single companion of similar size (a "binary").

The reason for choosing these parameters was that data published in this form (at least $\rho_{01}$ and $\rho_{11}$) are available for samples of radio-quiet elliptical and lenticular galaxies, other LLRG (with and without jets), and PRG (HCB, H86), allowing us to study the local galaxy density as a function of radio luminosity. HCB selected a radius of 100 kpc (equivalent to 133 kpc using $H_0 = 75$) since it includes galaxies that could have been interacting with the radio source over the last dynamical time scale ($\sim 10^8$ yr, assuming relative velocities $\lesssim 10^3$ km s$^{-1}$).

In Table 6 we list the environment parameters obtained from our images. Our observations cover in many cases a field smaller than 133 kpc. For these cases the field radius is given in the last column of Table 6. We did not measure the galaxy density parameters for the radio galaxies 1553+24 and 1736+32, since the CCD images of these objects have poor seeing and sensitivity. We have adopted the HCB criterion of considering only galaxy neighbors with sizes larger than 0.1 times that of the main galaxy to minimize contamination by background galaxies. Additional nuclei (revealed as secondary maxima) are considered as neighbors, but their sizes and those of the galaxies within the outline of the radio source are poorly estimated,

TABLE 6. Photometry and environment parameters.

| Name | $m_V$ | ± | $M_V$ | Aperture (arcsec) | $\rho_{00}$ | $\rho_{01}$ | $\rho_{10}$ | $\rho_{11}$ | Field (kpc) |
|---|---|---|---|---|---|---|---|---|---|
| 0034+25[a] | 13.35 | 0.07 | −22.19 | 59 | 6 | 1.8 | 12.5 | 4.6 | 104 |
| 0206+35[a] | 12.89 | 0.07 | −23.00 | 73 | 5 | 1.2 | 13.6 | 4.5 | 122 |
| 0836+29[b] | 14.26 | 0.06 | −23.24 | 120 | 4 | 0.9 | 8.3 | 1.9 | |
| 0836+29A | 15.45 | 0.03 | −21.76 | 63 | 1 | 0.3 | 1.6 | 0.5 | |
| 0844+31 | 13.92 | 0.07 | −23.38 | 120 | 6 | 0.8 | 11.4 | 1.6 | |
| 0908+37 | 15.67 | 0.04 | −22.65 | 65 | 4 | 0.8 | 7.1 | 1.4 | |
| 0915+32 | 15.12 | 0.04 | −21.99 | 42 | 1 | 1.2 | 3.1 | 3.7 | 85 |
| 1040+31 | 14.55 | 0.04 | −21.32 | 97 | 9 | 3.3: | 78.8 | 50: | 101 |
| 1243+26 | 15.07 | 0.05 | −22.88 | 50 | 7 | 1.9 | 15.9 | 3.9 | |
| 1254+27 | 12.30 | 0.09 | −22.74 | 204 | 2 | 0.3 | 3.5 | 0.5 | 69 |
| 1322+36 | 12.84 | 0.04 | −21.42 | 125 | 1 | 0.7 | 2.8 | 2.1 | 49 |
| 1357+28 | 14.81 | 0.04 | −22.33 | 77 | 3 | 0.8 | 5.4 | 1.7 | |
| 1450+28[c] | 16.31 | 0.08 | −22.47 | 41 | 4 | 3.0 | 9.6 | 8.4 | |
| 1521+28 | 15.09 | 0.05 | −22.68 | 77 | 6 | 1.2 | 7.5 | 1.5 | |
| 1525+29 | 14.95 | 0.08 | −22.27 | 100 | 7 | 4.9 | 12.1 | 11.9 | |
| 1528+29 | 15.35 | 0.07 | −22.47 | 63 | 3 | 1.2 | 3.8 | 1.5 | |
| 1553+24 | 14.41 | 0.05 | −21.84 | 63 | | | | | |
| 1637+29 | 14.97 | 0.07 | −22.94 | 64 | 3 | 0.5: | 14.8 | 2.9: | |
| 1643+27 | 15.77 | 0.06 | −22.49 | 62 | 4 | 1.5 | 6.9 | 2.4 | |
| 1658+30 | 14.70 | 0.04 | −21.11 | 65 | 2 | 0.9 | 3.4 | 1.5 | 98 |
| 1736+32[d] | 14.84 | 0.03 | −22.67 | 14 | | | | | |
| 1827+32 | 15.10 | 0.03 | −22.14 | 55 | 4 | 0.6 | 12.3 | 2.0 | 95 |
| 2116+26[b] | 11.86 | 0.06 | −22.22 | 217 | 0 | 0.0 | 0.0 | 0.0 | 53 |
| 2236+35[b] | 12.57 | 0.04 | −22.64 | 52 | 6 | 2.8 | 12.9 | 5.8 | 90 |

[a] Photometry from Paper I

[b] Photometry from Paper II

[c] We measured the total magnitude of this dumbbell galaxy and assigned a flux to the radio galaxy in proportion to its intensity peak. The given aperture corresponds to the total system.

[d] The galaxy is strongly contaminated by a bright star and we measured the total magnitude using the model constructed from the isophote analysis.

causing uncertainties in the parameters. In such cases the quantities are followed by the symbol ":" in Table 6.

Figure 4 shows the distribution of $\rho_{01}$ and $\rho_{11}$ for radio galaxies with three ranges of radio power, using the data by HCB, H86, and this work. First, (i) the group of all the radio-quiet elliptical and lenticular galaxies in the HCB sample ($N=46$); (ii) LLRG ($P_{eq}<10^{25}$ W Hz$^{-1}$) of the samples by HCB, H86, and this work ($N=66$); and finally, (iii) PRG ($P_{eq}>10^{25}$), 37 taken from H86 and another two from HCB. The galaxy density parameters for the LLRG in our sample 1254+27 and 1322+36 were also obtained by HCB and we have adopted their values since our observed field was only about half as large.

The histograms in Fig. 4 reveal the following results. Since the distributions of the environment parameters for our galaxies are not significatively different from those of the HCB and H86 samples, the histograms for LLRG have not changed appreciably after combining the three sam-

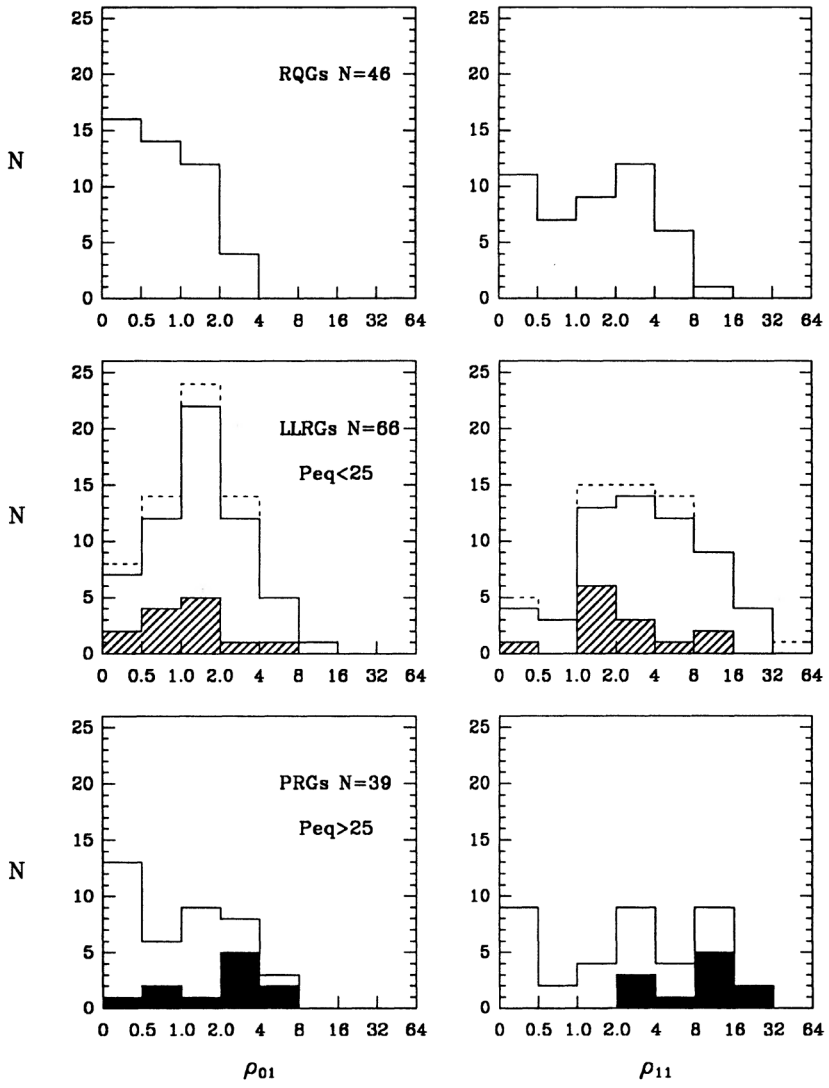


FIG. 4. Histograms of the local galaxy density parameters $\rho_{01}$ and $\rho_{11}$ for galaxies of different radio power (samples from HCB, H86, and this work). On the middle panel, the hatched region shows the sources measured in this work, the solid line is the combined distribution for this work and the literature, and dashed line includes the galaxies for which the measured parameters (this work) are lower limits. The shaded region on the bottom panel shows the FR I PRG of H86 and the solid line the combined distribution for PRG.

ples. Hence, we reach their same result that LLRG are located in regions of higher galaxy density and suffer stronger gravitational interaction than RQG. Although they form the group with smaller statistics, it appears that PRG have a wider range of values of $\rho_{01}$ and $\rho_{11}$, overlapping with those typically found for both RQG and LLRG. H86 confirmed, with their sample of PRG, the known relation between local galaxy density and Fanaroff–Riley, in the sense that FR II sources inhabit regions of lower galaxy density than FR I sources (Longair & Seldner 1979; Stocke & Perrenod 1981; Lilly & Prestage 1987). In Fig. 4 the FR I PRG of H86 are shown in the shaded area. The FR I PRG have $\rho_{01}$ and $\rho_{11}$ values similar to LLRG, which typically belong to FR I class. The remaining PRG in Fig. 4 have local galaxy densities similar to RQG. Summarizing the results of these comparisons, it is confirmed that LLRG tend to be located in regions of high local galaxy density at a larger rate than RQG and PRG, and that the local galaxy density strongly influences the FR class, in the sense that a radio galaxy in a high density region tends to be of FR I class (see also Prestage & Peacock 1988).

In Fig. 5 we plot the linear size of the jets ($L_{\rm jet}$) versus the total radio power. Our aim is to investigate the possible

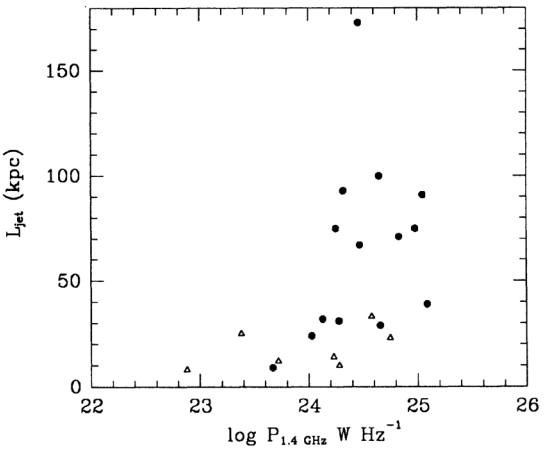


FIG. 5. Linear size of the radio sources vs total radio power. Triangles correspond to sources with $\rho_{11} \gtrsim 4$.

relation, in the range of radio luminosity of our sample, between radio power, environment and jet size. We find that *all* sources with $P_{1.4} \lesssim 10^{24.2}$ W $Hz^{-1}$ have jet sizes $\lesssim 40$ kpc, and that 50% of sources with higher luminosity have jet sizes $>40$ kpc whereas the remaining 50% have jets shorter than this value. In addition, *all* sources in dense environments ($\rho_{11} \gtrsim 4$) have short radio jets ($L_{jet} \lesssim 40$ kpc) irrespectively of their radio power. The density of the environment seems to be, therefore, an important parameter in determining the size of the jet, in the sense that in high density regions radio sources are unable to form large jets. In less dense regions the jet size is controlled by the radio power: high radio power implies large jets ($\gtrsim 40$ kpc).

This effect is what we would expect in view of the correlation found by Morganti *et al.* (1988) between linear size and central density of the surrounding hot gas, as determined from x-ray observations of B2 radio sources. The parameter $\rho_{11}$ is related to the gravitational potential at the radio source due to its neighbors. The potential determines the distribution of the intracluster/intergalactic gas and, consequently, the central density. Therefore, high values of $\rho_{11}$ are directly indicating high central gas densities.

### *4.3 Galaxy Interactions/Mergers*

There is a group of eight galaxies in our sample that likely belong to interacting systems. These galaxies are 0034+25, 0206+35, 0915+32, 1243+26, 1322+36, 1450+28, 1525+29, and 2236+35, and in all cases the companion galaxy(ies), in general of about the same size as the radio galaxy, are identified on our images. B2 0034+25 and B2 0206+35 (see Paper I), together with 1525+25, show, clearly, evidence for interaction in the sense that they and their companions exhibit isophote distortions. In particular 1525+29 and its companion have a small velocity difference (Valentijn & Casertano 1988). This galaxy and 1450+28 are dumbbell systems. B2 1322+36 (NGC 5141) is one of the components of a known bright binary (Soares 1989) where the secondary component (NGC 5142) shows isophote distortions. B2 0915+32 has a nearby spiral and its radio morphology suggests interaction. B2 1243+26 has optical morphological indications of gravitational interaction with their companions and the distortion of its radio jet suggests also an encounter. B2 2236+35 has two nearby ellipticals with isophote twisting and extended envelopes, and presents itself isophote twisting in the direction of one of them. The S-shaped morphology of the radio emission of this source is also indicative of a gravitational encounter (Paper II).

Other three galaxies, namely 0836+29, 1637+29, and 1040+31, have extended secondary maxima within their envelopes and they are probably interacting systems or remnants of past mergers. The secondary maxima of 1637+29 is in fact another galaxy (de Ruiter *et al.* 1988) and the authors suggest that these two galaxies are interacting in view of the peculiar morphology of the radio jet. This is also supported by the presence of faint shells around 1637+29 revealed in our *R* image. Although some of the remaining 13 objects in our sample are located in rich regions, none of them appears to be interacting with a particular neighbor. However, some sources exhibit peculiar morphologies in the optical (dust, boxiness, disky isophotes, extended envelopes, cD morphology) or in the radio (particular symmetry of the jets) that are generally attributed to past interaction/merger processes. These sources are 4C29.30, 1254+26, 1322+36, 1521+28, 1528+29, 1658+30, 1827+32, and 2116+26.

In summary, we find that a large fraction of LLRG with radio jets (45%–75%) shows direct or indirect evidence of ongoing or past interaction/merging processes. A similar result was obtained by H86 for their sample of PRG. These authors specifically found peculiar optical morphologies in the form of tails, shells, and bridges, which are considered as characteristic signatures of collisions involving, at least, one gas-rich system (Toomre & Toomre 1972). The presence of a gas-rich system was moreover reinforced by the fact that PRG with such peculiar morphologies have enhanced line emission and are located in regions with low galaxy density. Only two objects in our sample, namely 0836+29A (4C29.30) and 1637+29, have peculiar optical morphologies suggesting interactions with gas-rich systems. 4C29.30 exhibits also strong line emission and is a far infrared emitter detected by *IRAS*. B2 0915+32 could be also interacting with a spiral galaxy. The low detection rate of interactions involving gas-rich systems among LLRG with radio jets is consistent with their location in regions with high galaxy density, where the proportion of spiral versus elliptical galaxies is low.

### *4.4 Are Low Luminosity Radio Galaxies the Progenitors of cD Galaxies?*

It has been stressed that LLRG with FR I morphology are associated with giant elliptical or cD galaxies and are located in similar environments (H86; SH; Lilly & Prestage 1987; Owen & Laing 1989). We have confirmed

that LLRG FR I sources inhabit regions of high local galaxy density and have similar luminosities to bright cluster galaxies, although not all the galaxies in our sample lie at the center of clusters. The presence of extended envelopes, multiple nuclei, and x-ray emission in sources in our sample is indicating a cD-like population of galaxies, although from our surface brightness data we have been able to classify firmly only three cD galaxies.

The origin of cD galaxies is still under debate, although a natural possibility is that they formed from galaxy interactions: merging, accretion, and stripping (Gallagher & Ostriker 1972; Ostriker & Tremaine 1975; Richstone 1976). Our data reveal a high fraction of luminous galaxies undergoing interaction or merging in relatively dense environments, with overall properties very similar to those of cD galaxies. All these facts bring us to suggest that this population of galaxies may represent *the precursors of cD galaxies,* in the sense that, in general, a galaxy located in an environment like that of LLRG with jets may evolve to build a cD galaxy through encounters and mergers. These processes could be, at the same time, the triggers of the radio emission of those galaxies, although this should be tested with observations of a sample of radio-quiet ellipticals of the same absolute magnitudes.

## 5. CONCLUSIONS

We have presented a morphological description and new photometric information for a sample of 24 low luminosity radio galaxies with radio jets. We confirm that FR I LLRG are intrinsically more luminous in the optical than powerful radio galaxies, and inhabit regions of higher galaxy density than radio-quiet ellipticals and powerful radio sources.

From our analysis it appears that both the total radio power and the environment play a role in determining the jet size. Large jets are present only in the powerful radio galaxies, but the lack of large jets in high density regions suggests an effect of the environment.

From the analysis of the brightness profiles we have measured the effective radius ($r_e$) and effective surface brightness ($\mu_e$) for the galaxies of the sample. We do not find significative differences on the $\mu_e$–$r_e$ relation between LLRG with jets, PRG, normal ellipticals, and BCG. We find, however, that a significant fraction of the profiles are typical of cD galaxies, showing excesses in the outer parts.

A high fraction of the objects (75%) have morphological peculiarities that can be associated with indicators of either recent merger processes or gravitational interaction, as occurs for powerful radio sources (H86). The difference with PRG is that these objects interact with gas-rich systems, while LLRG interact with gas-poor galaxies. This conclusion has been reached on the basis of the presence of radio and optical morphological peculiarities and/or identification of close pairs of similar size, sometimes with available radial velocity information.

The fact that our results are, in general, consistent with H86 and SH may imply that there are not significant differences between LLRG with and without radio jets, although a more detailed analysis must be done. In particular, similar observations of LLRG without radio jets, selected with the same criteria that were used for the present sample, will be very useful to understand the properties of the extragalactic radio-source population. Also, a comparison of the properties of the present sample with that of radio-quiet ellipticals with similar absolute magnitudes is needed to interpret the fractions of the radio galaxies that have morphological peculiarities.

We propose finally, that the host galaxies of low luminosity radio sources with jets could form cD galaxies. Although we cannot *firmly* identify a high fraction of the objects as cD galaxies, the overall optical properties of the galaxies (luminosity and morphology) and the density of their environments, suggest that LLRG are evolving, through mergers and interactions, to build a cD galaxy.

J.I.G.-S. was partly supported by the Kapteyn Astronomical Institute, the Instituto de Astrofísica de Canarias, and by the DGYCIT project PB89-0375-C02-02. J.I.G.-S. and R.C. acknowledge their fellowships of the Spanish Ministry of Education and Science. We wish to thank M. Balcells for obtaining some of the data at the INT during a service night. We also thank the referee for his/her valuable comments and suggestions. The WHT and INT telescopes are operated by the RGO at the Spanish Observatorio del Roque de los Muchachos of the Instituto de Astrofísica de Canarias on behalf of the Science and Engineering Research Council of the United Kingdom and the Netherlands Organization for Scientific Research (NWO).

## REFERENCES

Baum, S. A., & Heckman, T. M. 1989a, ApJ, 336, 681
Baum, S. A., & Heckman, T. M. 1989b, ApJ, 336, 702
Bender, R., Döbereiner, S., & Möllenhoff, C. 1987, A&A, 177, L53
Bender, R., Surma, P., Döbereiner, S., Möllenhoff, C., & Medejsky, R. 1989, A&A, 217, 35
Binney, J., & Petrou, M. 1985, MNRAS, 214, 449
Blandford, R. D., & Icke, V. 1978, MNRAS, 185, 527
Bruzual, G. A. 1983, RMxA&A, 8, 63
Burstein, D., & Heiles, C. 1982, AJ, 84, 1478
Cawson, M. 1983, Ph.D. thesis, University of Cambridge
Colina, L., & Pérez-Fournon, I. 1990a, ApJS, 72, 14
Colina, L., & Pérez-Fournon, I. 1990b, ApJ, 349, 45
Colla, G., *et al.* 1975, A&AS, 20, 1
Davies, R. L., & Illingworth, G. 1983, ApJ, 266, 516
de Ruiter, H. R., Parma, P., Fanti, C., & Fanti, R. 1986, A&AS, 65, 111
de Ruiter, H. R., Parma, P., Fanti, R., & Ekers, R. D. 1988, ApJ, 329, 225
Fanaroff, B. L., & Riley, J. M. 1974, MNRAS, 167, 31P
Fanti, R., Gioia, I., Lari, C., & Ulrich, M. H. 1978, A&AS, 34, 341
Fanti, C., *et al.* 1983, A&AS, 51, 179
Fanti, C., Fanti, R., de Ruiter, H. R., & Parma, P. 1986, A&AS, 65, 145
Fanti, C., Fanti, R., de Ruiter, H. R., & Parma, P. 1987, A&AS, 69, 57
Gallagher, J. S., & Ostriker, J. P. 1972, AJ, 77, 288
González-Serrano, J. I., & Pérez-Fournon, I. 1989, ApJ, 338, L29

González-Serrano, J. I., & Pérez-Fournon, I. 1991, A&A, 249, 75 (Paper I)
González-Serrano, J. I., & Pérez-Fournon, I. 1992, AJ, 104, 535 (Paper II)
Heckman, T. M., Carty, T. J., & Bothun, G. D. 1985, ApJ, 288, 122 (HCB)
Heckman, T. M., *et al.* 1986, ApJ, 311, 526 (H86)
Hine, R. G., & Longair, M. S. 1979, MNRAS, 188, 111
Hoessel, J. G., Oegerle, W. R., & Schneider, D. P. 1987, AJ, 94, 1111
Kormendy, J. 1980, in Two Dimensional Photometry, ESO Workshop, edited by P. Crane and K. Kjär (ESO, Garching), p. 191
Lilly, S. J., & Prestage, R. M. 1987, MNRAS, 225, 531
Longair, M. S., & Seldner, M. 1979, MNRAS, 189, 433
Morganti, R., Fanti, C. Fanti, R., Parma, P., & de Ruiter, H. R. 1987, A&A, 183, 203,
Morganti, R., Fanti, R., Gioia, I. M., Harris, D. E., Parma, P., & de Ruiter, H. R. 1988, A&A, 189, 11
Morganti, R., Ulrich, M.-H., & Tadhunter, C. N. 1992, MNRAS, 254, 546
Nieto, J.-L., & Bender, R. 1989, A&A, 215, 266
Ostriker, J. P., & Tremaine, S. D. 1975, ApJ, 202, L113
Owen, F. N., & Laing, R. A. 1989, MNRAS, 238, 357
Parma, P., Ekers, R. D., & Fanti, R. 1985, A&AS, 59, 511
Parma, P., de Ruiter, H. R., Fanti, C., & Fanti, R. 1986, A&AS, 64, 135
Parma, P., Fanti, C., Fanti, R., Morganti, R., & de Ruiter, H. R. 1987, A&A, 181, 244
Prestage, R. M., & Peacock, J. A. 1988, MNRAS, 230, 131
Richstone, D. O. 1976, ApJ, 204, 642
Sandage, A. 1972, ApJ, 178, 25
Schombert, J. M. 1986, ApJS, 60, 603
Smith, E. P., & Heckman, T. M. 1989a, ApJS, 69, 365
Smith, E. P., & Heckman, T. M. 1989b, ApJ, 341, 658 (SH)
Soares, D. S. L. 1989, Ph.D. thesis, University of Groningen
Stocke, J. T., & Perrenod, S. C. 1981, ApJ, 245, 375
Toomre, A., & Toomre, J. 1972, ApJ, 178, 623
Valentijn, E. A., & Casertano, S. 1988, A&A, 206, 27
van Breugel, W. J. M., Heckman, T. M., Miley, G. K., & Flilppenko, A. V. 1986, ApJ, 311, 84